Thermospheric Flows at Jupiter for Differing Solar Wind Conditions

Nicholas Achilleos[1]

[1]Department of Physics and Astronomy, [2]Mullard Space Science Laboratory (both part of the Centre for Planetary Sciences), University College London, UK

Contact: nick@apl.ucl.ac.uk

Download Poster: http://www.homepages.ucl.ac.uk/∼ucapnac/posters/nach_epsc_2009.pdf

Acknowledgement: We wish to thank Dr. Chris Smith, who developed the thermosphere-magnetosphere code used for this preliminary study.

September 14–18, 2009

Abstract

The magnetosphere-ionosphere coupling at Jupiter is known to play a central role in generating auroral emissions at this planet. The strength of these emissions is partly determined by the relative rotational flows in the upper atmosphere (thermosphere) and in the magnetodisc. We present simulations of the atmospheric flow which employ an azimuthally symmetric global circulation model. In order to make preliminary estimates of the effects of upstream solar wind conditions on these flows, we calculate models which assume different profiles of magnetic field and plasma angular velocity in the magnetodisc, corresponding to compressed and expanded states of the planet's magnetosphere. We use these simulations to comment on the relationship between global magnetospheric configuration and the global pattern of winds and energy inputs into the thermosphere.

Introduction

- Much progress has been made towards a full understanding of the nature of magnetosphere-ionosphere (M-I) coupling at Jupiter, and the link between this process and the field-aligned currents which drive this planet's auroral emissions (e.g. [4, 1, 6, 2, 8, 7]).
- Such studies have emphasised *rotational dynamics*: Magnetic field-aligned current density $\boldsymbol{J}_{||}$ which links ionosphere-thermosphere and magnetosphere is a signature of the differential rotation between these regions. This difference arises as disc plasma diffuses radially outward - the magnetic field decreases with distance and becomes less effective at maintaining disc–planet co-rotation.
- The full time-dependent problem of M-I coupling is very challenging. The steady-state formulation of the disc plasma's equation of motion (Hill-Pontius Equation), has been vital for progress in this area. Here we give the form of this equation derived by [8], who assumed azimuthal symmetry about the magnetic / rotation axis:

$$\frac{1}{\rho_e}\frac{d(\rho_e^2\,\Omega_M)}{d\rho_e} = \frac{8\pi\Sigma_P F_e B_{ze}(\rho_e)}{\dot{M}}\,(\Omega_T - \Omega_M), \qquad (1)$$

where Ω_M denotes angular velocity of magnetospheric flux tube (field line) with equatorial values of crossing distance ρ_e and magnetic field B_{ze}; Ω_T is effective angular velocity of the neutral thermosphere located at the footpoint of the flux tube; Σ_P is height-integrated Pedersen conductivity of the ionosphere; F_e is the magnetic flux function, whose value is constant all the way along a flux tube / field line; and $\dot{M}$ is the integrated mass of plasma flowing radially through the disc per unit time.

Model Inputs and Definitions

- $1\,R_J$ = Jupiter radius = 71492 km
- $1\,P_J$ = Jupiter rotation period = 9.84 hr
- ρ_D = outer disc radius
- Figure 1 :Magnetospheric Field : We performed calculations using the model of [8] with the two equatorial magnetic field profiles shown here, representing compressed ($\rho_D = 60\,R_J$) and expanded conditions ($\rho_D = 90\,R_J$) for the Jovian magnetosphere:

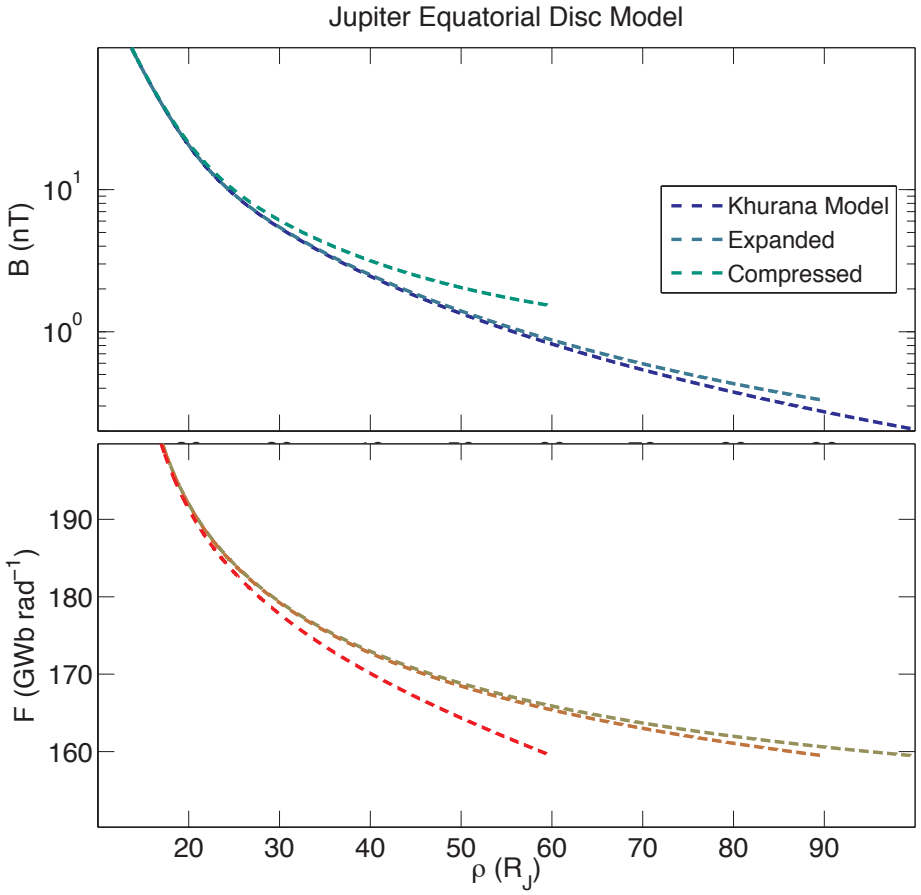

- Both field profiles were simply obtained by conserving the total magnetic flux through the equatorial plane of the empirical field model by [5]. The flux function F represents magnetic flux which threads the region between a given shell of field lines and infinite radial distance from the planet ($F = 0$ at magnetic poles).

Model Inputs and Definitions, cont.

- Models for both magnetospheric configurations were run for 50 simulated planet rotations (50 P_J) in order to reach steady state. Simulated time step used was $\Delta_t = 3$ sec. The axisymmetric model is 2D (latitude, pressure level) and one 50-rotation run required $\sim$2.5 CPU hours on an Apple MacBook Pro with Intel Core 2 Duo Processor (2.33 GHz).
- To capture thermospheric dynamics and heating, the model solves the time-dependent Navier-Stokes equations of fluid flow, assuming a spherical shell geometry for the hydrogen-rich thermosphere.
- To capture magnetospheric dynamics at each time step, the model updates the values of Ω_T used in solving Eq. (1) for steady-state plasma flow. Thus a final profile of Ω_M is produced which is also consistent with thermospheric conditions, and a final profile of Ω_T is produced which is consistent with the strong magnetospheric forcing of the auroral thermosphere, i.e. the atmospheric region magnetically conjugate to the equatorial plasmadisc.

Figure 2: High-Latitude Flows and Conductivity

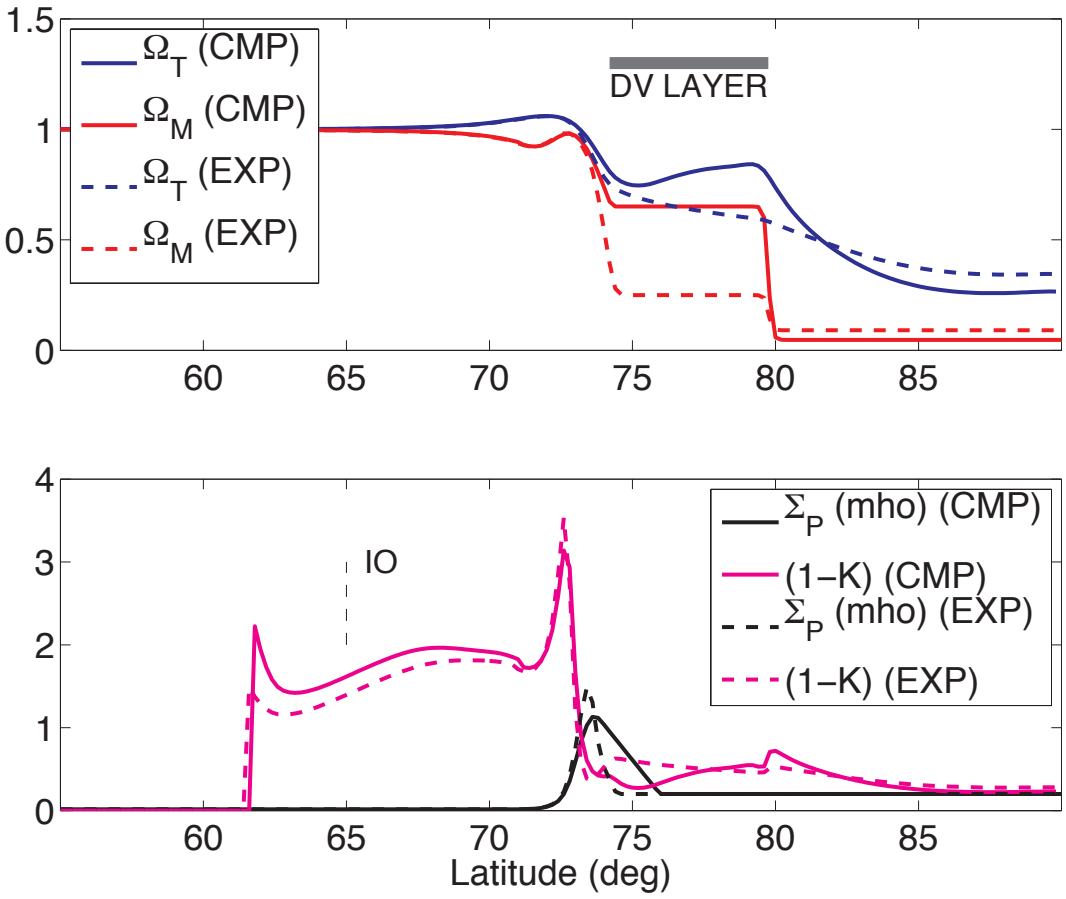

- High-latitude ionospheric profiles for various parameters are shown for both compressed and expanded magnetodisc configurations. The labelled positions of the Io footprint and the Dungey-Vasyliunas (DV) layer enclose the region conjugate to the disc. The higher field strength for the compressed model maintains higher Ω_M and Ω_T in the outer disc solutions (these are expressed in units of Ω_J, the planetary angular velocity). The Ω_M values in the DV layer were specified *a priori* by conserving angular momentum in the DV model region of [6]. We confirm regions of super-rotating Ω_N, as originally found by [8].
- The peak in Σ_P for both models occurs at the main auroral oval (conjugate to the outer disc). Σ_P for the polar cap (poleward of the DV layer) must be specified *a priori*, while the profile for the DV layer is constrained to smoothly connect the disc and cap. The slippage parameter $(1-K) = \frac{\Omega_T - \Omega_M}{\Omega_J - \Omega_M}$.

Figure 3: Meridional Flow, Compressed Model

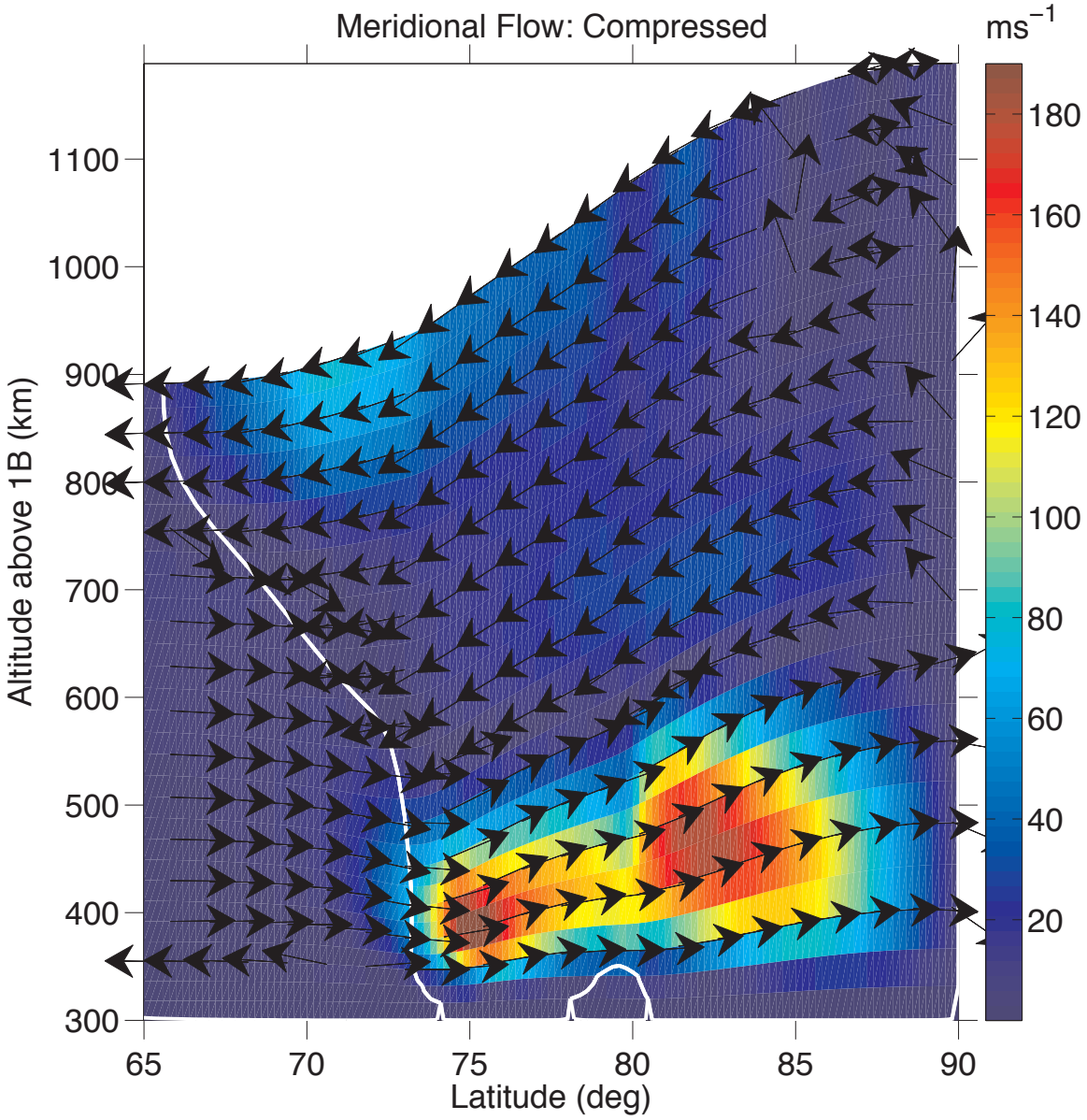

The colour scale shows magnitude of the meridional velocity component as a function of latitude and altitude in the 'compressed' model's polar region. The arrows show velocity direction. We see the flow pattern described by [8]: A pole-to-equator flow at high altitude, with flow of reverse direction at low altitude. The white contour shows locus for planetary corotation of neutral gas, and runs near the low-altitude location of the main auroral oval. The localised accelerated flows in the DV layer and polar cap are evident.

Figure 4: Meridional Flow, Expanded Model

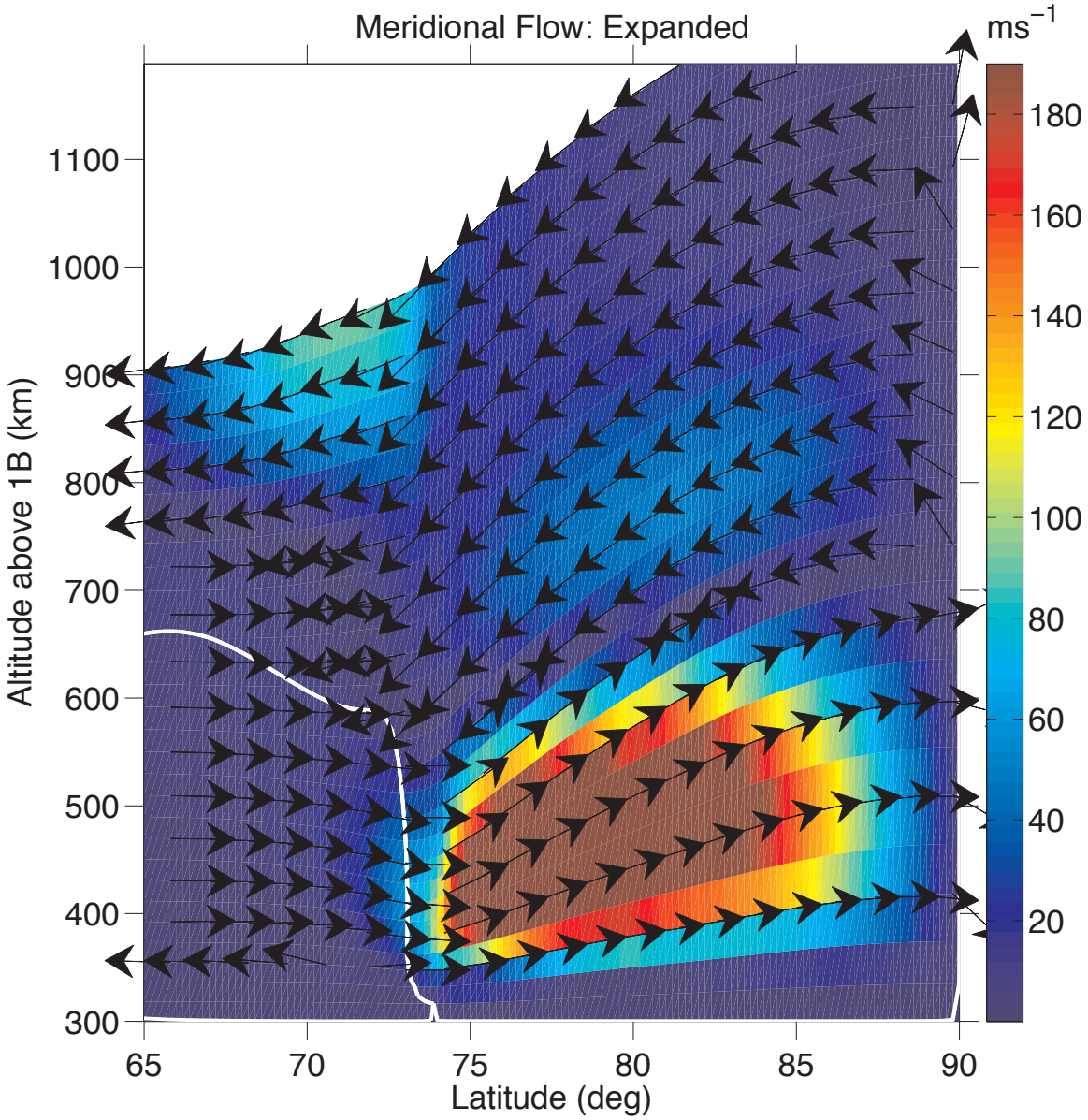

As for Figure 3, but for the output of the expanded magnetodisc simulation. The localised rapid flows poleward of the low-altitude auroral oval are more strongly accelerated than in the compressed model. This is partly due to the compressed model's *smaller* shear between thermospheric and magnetospheric angular velocities, which leads to weaker auroral activity and heating.

Figure 5: Azimuthal Flow, Compressed Model

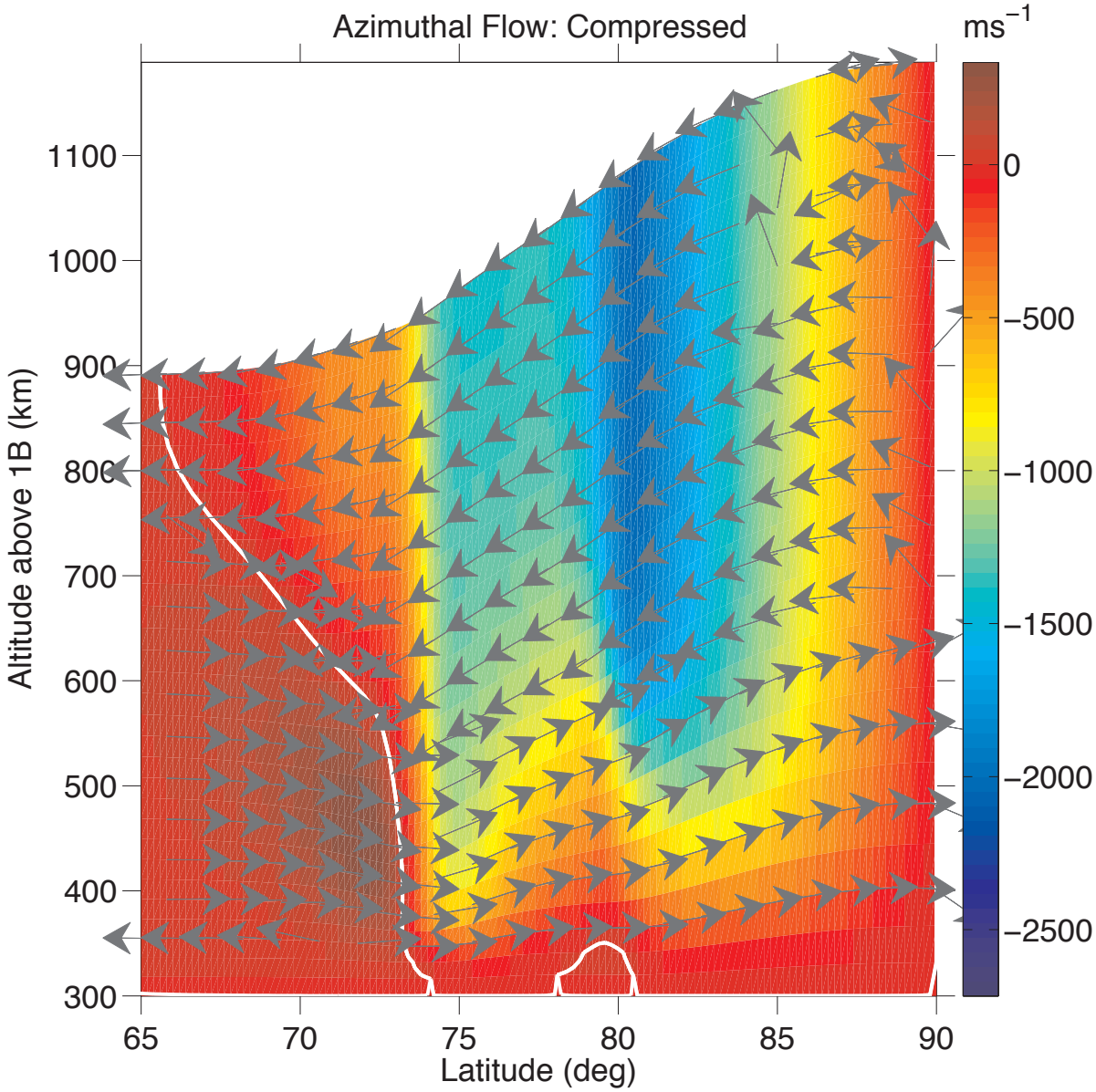

Azimuthal velocity V_ϕ in the corotating frame of the compressed model (i.e. positive (negative) values on the colour scale correspond to super- (sub-)corotation). Zero V_ϕ (i.e. corotation with planet) is shown as a white contour. Meridional velocity directions are shown as for previous Figures. The signature of lower Ω_T in the polar cap is evident. The region at latitude 77–80°, 350–500 km shows a local maximum in V_ϕ; this is due to the strong gradient in meridional velocity at the low-latitude edge of this region (Figure 3) driving a relatively efficient poleward transport of angular momentum. The highest levels of super-corotation for the neutral thermosphere are seen just equatorward of the auroral oval location near 73° latitude.

Figure 6: Azimuthal Flow, Expanded Model

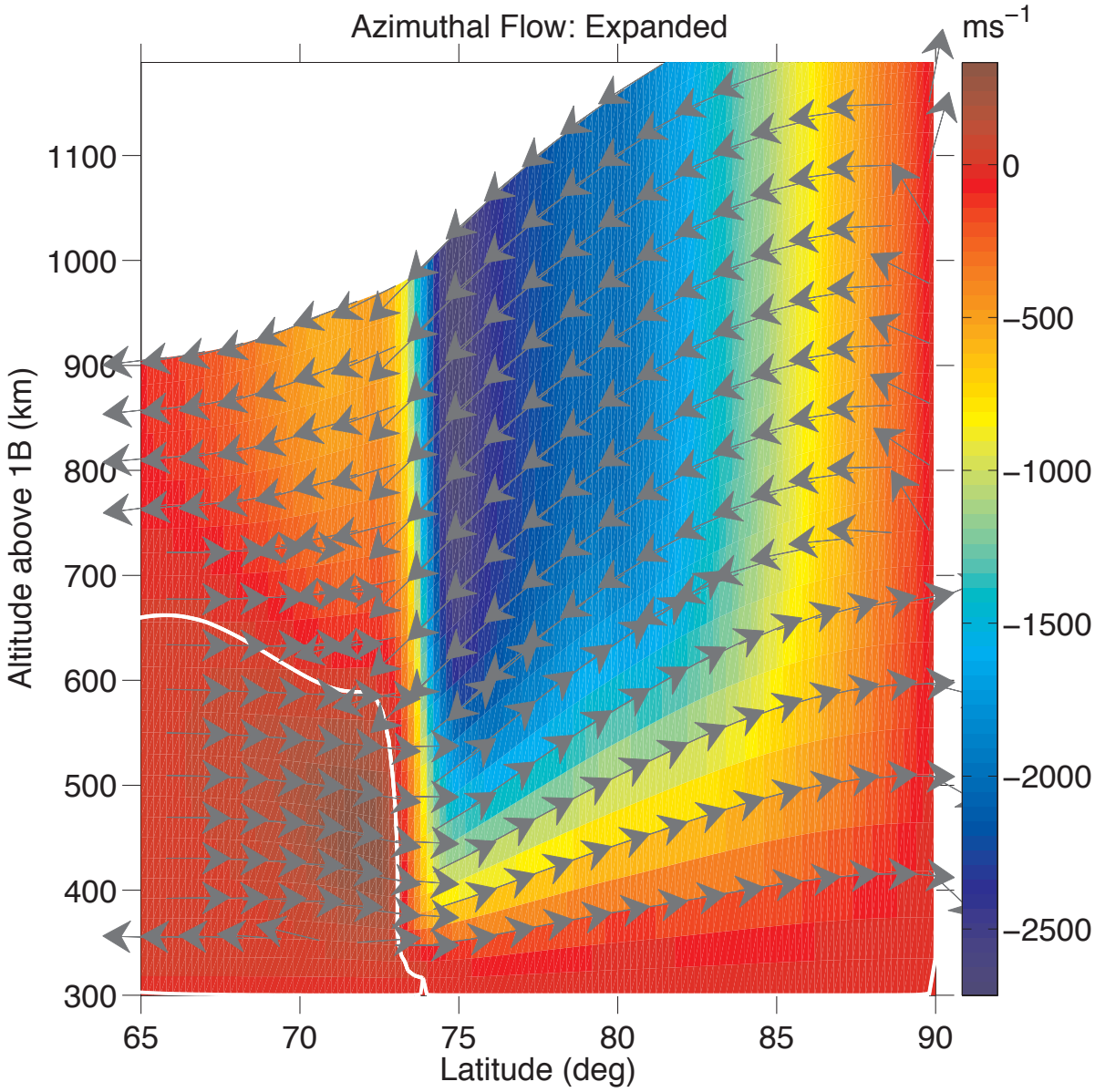

As for Figure 5, but for expanded magnetodisc configuration. Here, meridional flow speed shows a less 'structured' transition between DV layer and cap (compare Figures 3 and 4). More monotonic transition is seen for V_ϕ going from main auroral oval to the DV layer, to the polar cap. V_ϕ in the DV layer is more negative than for the compressed model, mainly due to the lower Ω_M assumed for this region in the expanded model.

The detailed structure of these high-latitude flow patterns influences field-aligned current, and thus has consequences for the brightness and form of polar auroras.

Figure 7: Temperature, Compressed Model

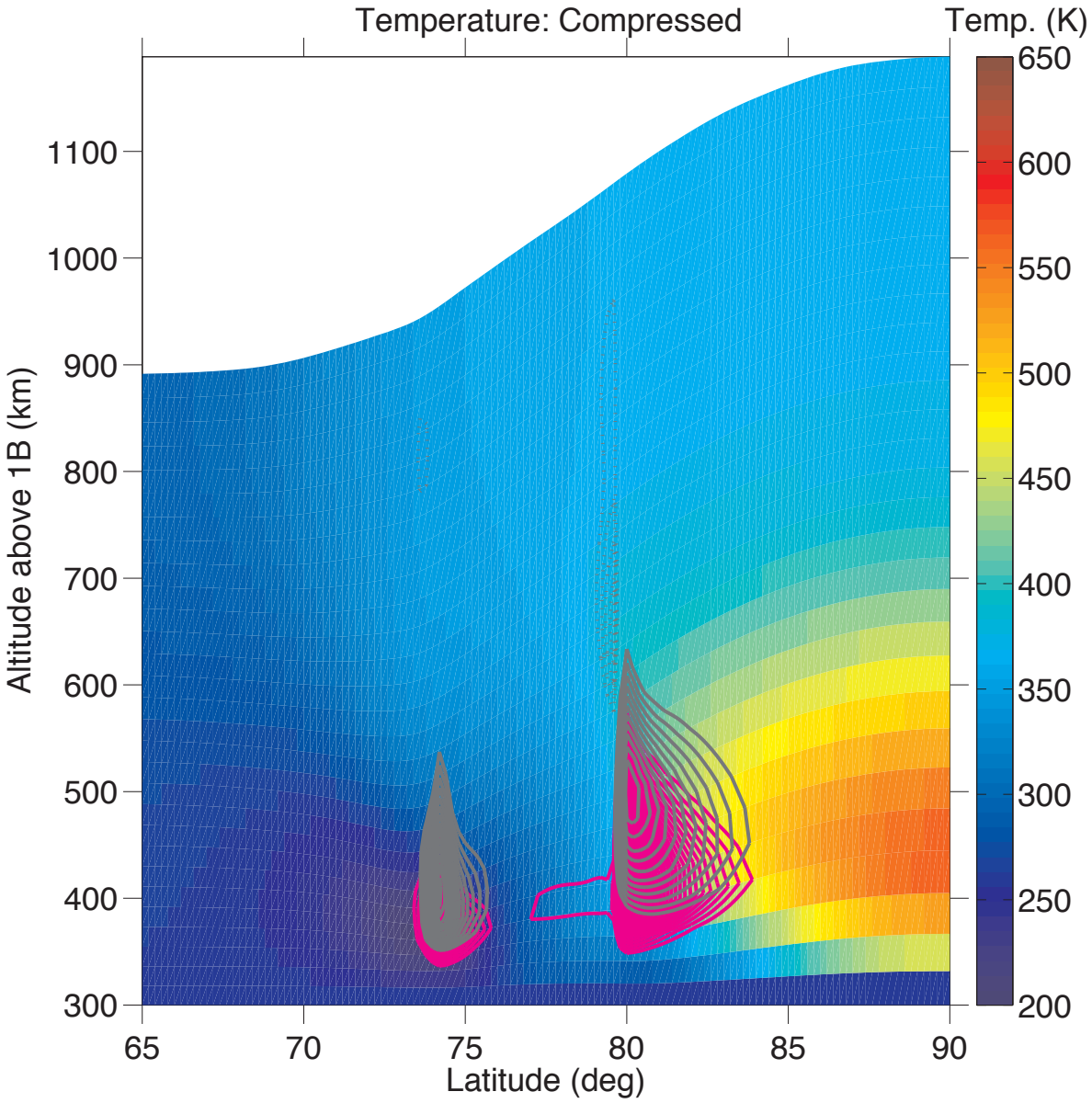

Temperature distribution for the compressed model on a colour scale. Magenta contours show regions where Joule heating exceeds $20\,\mathrm{Wkg}^{-1}$. Solid grey contours show regions where ion drag increases kinetic energy (i.e. acts to decrease Ω_T in the inertial frame) at a rate $> 20\,\mathrm{Wkg}^{-1}$; while dotted grey contours indicate where ion drag is decreasing kinetic energy at $< -20\,\mathrm{Wkg}^{-1}$. The altitude of these maximum positive energy inputs is partly controlled by the vertical profile of conductivity, for which we use an adapted form of the auroral thermospheric structure by [3]. These same peak energy inputs occur at the locations of highest shear between Ω_T and Ω_M (see Figure 2).

Figure 8: Temperature, Expanded Model

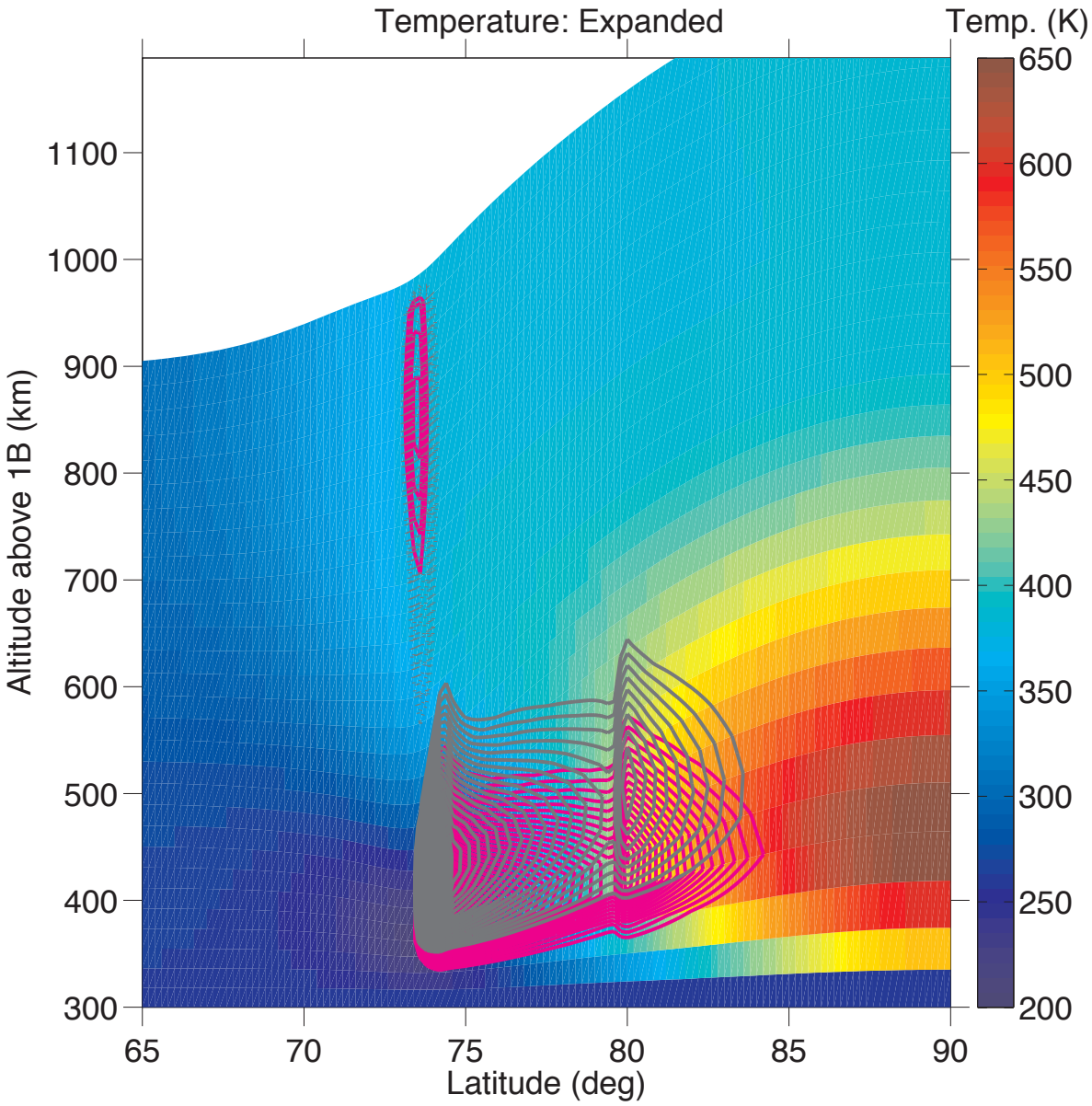

As for Figure 7, but for the expanded magnetodisc. The highest temperatures here are about $\sim$ 100 K higher than for the compressed model. Strong poleward transport of heat energy is achieved. The peak Joule heating and ion drag regions are shown, as for Figure 7. Compared to the compressed model, the expanded model has a more extensive spatial region of strong Joule heating and ion drag; this aspect is largely controlled by the global shear between magnetospheric and thermosperic angular velocity. We therefore expect generally higher levels of auroral activity and brightness for an expanded magnetosphere. As discussed in Figures 5 and 6, the detailed form of the polar flows is quite distinct for different magnetospheric configurations. Further study of this aspect may thus provide an important diagnostic for magnetospheric state, based on the morphology of the polar auroras.

References

[1] S. W. H. Cowley, E. J. Bunce, and J. D. Nichols. Origins of Jupiter's main oval auroral emissions. *Journal of Geophysical Research (Space Physics)*, 108:8002, January 2003.

[2] S. W. H. Cowley, J. D. Nichols, et al. Modulation of jupiter's plasma flow, polar currents and auroral precipitation... *Ann. Geophys.*, 25:1433–1463, 2007.

[3] D. Grodent and J.-C. Gérard. A self-consistent model of the Jovian auroral thermal structure. *J. Geophys. Res.*, 106:12933–12952, July 2001.

[4] T. W. Hill. The Jovian auroral oval. *J. Geophys. Res.*, 106:8101–8108, May 2001.

[5] K. K. Khurana. Influence of solar wind on Jupiter's magnetosphere deduced from currents in the equatorial plane. *J. Geophys. Res.*, 106:25999–26016, November 2001.

[6] J. D. Nichols and S. W. H. Cowley. Magnetosphere-ionosphere coupling currents in Jupiter's middle magnetosphere: effect of magnetosphere-ionosphere decoupling by field-aligned auroral voltages. *Ann. Geophys.*, 23:799–808, March 2005.

[7] D. H. Pontius. Radial mass transport and rotational dynamics. *J. Geophys. Res.*, 102:7137–7150, April 1997.

[8] C. G. A. Smith and A. D. Aylward. Coupled rotational dynamics of Jupiter's thermosphere and magnetosphere. *Ann. Geophys.*, 27:199–230, January 2009.